ACS POLYMERS Au
AN OPEN ACCESS JOURNAL OF THE AMERICAN CHEMICAL SOCIETY

pubs.acs.org/polymerau
Article

Amino-Acid-Derived Anionic Polyacrylamides with Tailored Hydrophobicity—Physicochemical Properties and Cellular Interactions

Jonas De Breuck, Michael Streiber,[⊥] Michael Ringleb,[⊥] Dennis Schröder, Natascha Herzog, Ulrich S. Schubert, Stefan Zechel, Anja Traeger, and Meike N. Leiske*

Cite This: ACS Polym. Au 2024, 4, 222−234
Read Online

ACCESS | Metrics & More | Article Recommendations | Supporting Information

ABSTRACT: Polyanions can internalize into cells via endocytosis without any cell disruption and are therefore interesting materials for biomedical applications. In this study, amino-acid-derived polyanions with different alkyl side-chains are synthesized via postpolymerization modification of poly(pentafluorophenyl acrylate), which is synthesized via reversible addition−fragmentation chain-transfer (RAFT) polymerization, to obtain polyanions with tailored hydrophobicity and alkyl branching. The success of the reaction is verified by size-exclusion chromatography, NMR spectroscopy, and infrared spectroscopy. The hydrophobicity, surface charge, and pH dependence are investigated in detail by titrations, high-performance liquid chromatography, and partition coefficient measurements. Remarkably, the determined pK_a-values for all synthesized polyanions are very similar to those of poly(acrylic acid) (pK_a = 4.5), despite detectable differences in hydrophobicity. Interactions between amino-acid-derived polyanions with L929 fibroblasts reveal very slow cell association as well as accumulation of polymers in the cell membrane. Notably, the more hydrophobic amino-acid-derived polyanions show higher cell association. Our results emphasize the importance of macromolecular engineering toward ideal charge and hydrophobicity for polymer association with cell membranes and internalization. This study further highlights the potential of amino-acid-derived polymers and the diversity they provide for tailoring properties toward drug delivery applications.

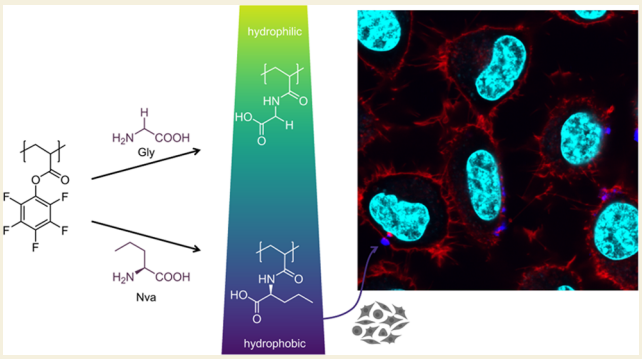

KEYWORDS: *polycarboxylate, amino-acid-derived polymer, polyanion, polyelectrolyte, biomimicking polymer, postpolymerization modification, cell association*

1. INTRODUCTION

During the last decades, the application of (polymeric) nanocarriers became an essential asset for drug delivery, therapeutic, and diagnostic systems.[1] To increase the therapeutic efficiency, it is important not only to repress undesired interactions with cells and tissue but also to induce a targetability to specific cells.[2] Recently, significant effort was made to incorporate tissue-targeting motifs into polymeric nanocarriers to increase their specificity.[3−6] Their performance was shown to highly depend on several physiochemical properties of the nanocarriers, such as its shape, size, charge, and hydrophobicity.[7]

The intracellular delivery of therapeutic biomacromolecules such as nucleic acids or peptides is of critical importance for their therapeutic efficiency. Owing to their size, charge, and inherent instability, biomacromolecules often need to be encapsulated for more stability and enhanced cellular uptake via endocytic pathways for intracellular delivery of drugs as they are impermeable to the cell membrane. After membrane engulfment, referred to as endocytosis, a rapid release of the therapeutics (i.e., endosomal escape) is required to minimize degradation and maximize therapeutic efficiency.[8] Over the years, various pH-responsive materials have been investigated regarding their endosomal escape property. pH-responsive polymers are protonated during endosomal maturation, as the pH value of the extracellular physiological environment (bloodstream: pH = 7.4) differs from the endosomal pH value (5.0−6.8). Biocompatible, biodegradable, and amphiphilic polypeptides have shown a pH-dependent membrane-permeabilizing capability due to their pH-responsive amines or carboxylic acid groups.[9] Besides, synthetic alternatives, which

Received: November 29, 2023
Revised: February 7, 2024
Accepted: February 8, 2024
Published: March 12, 2024

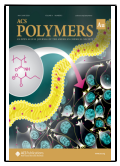

are often more cost-effective compared with peptides, have attracted attention in the past.[10−12] pH-responsive polymers are polyelectrolytes and can carry anionic (polyanions) or cationic (polycation) dissociable groups. Polycations (i.e., poly(ethylene imine)s) are known for their buffer capacity and protonation inside endosomal compartments, which is linked to its potential to cross these after acidification resulting in osmotic swelling, also discussed as the proton sponge effect.[13] Furthermore, strong interactions with the endolysosomal membrane have been described to facilitate the release of therapeutics by pore formation.[14] Here, a slightly acidic pK_a-value of the polymeric amine is desirable in order to promote endosomal membrane interaction under acidic conditions, but at the same time to minimize interactions with the cytoplasmic membrane to improve the compatibility of the polycations.[10] This high membrane interaction further renders them suitable for applications as antimicrobial polymers.[15,16]

In contrast, polyanions are often formed of polycarboxylates, that are negatively charged at the physiological pH value of blood (pH = 7.4) and, consequently, do not penetrate negatively charged cell membranes due to repulsive interactions.[8] However, their pH-induced protonation and loss/reduction of anionic character can cause endosomal membrane disruption. To this end, the pH response of polyanions (i.e., the pK_a-value) often takes place at physiologically relevant pH values (i.e., pH = 4−6),[8] making them an attractive alternative to polycations, which often feature a higher pK_a-value outside the physiological range (i.e., pH = 7−9).[17] Below the pK_a, the increased membrane interaction of polyanions is attributed to less ionic repulsion between polymers and the cell membrane, which is also facilitated by their increased hydrophobicity in the nonionic state. Consequently, the pH-dependent endosomolytic activity of polyanions is generally considered less harmful, as they are unlikely to be internalized into cells via translocation of the synthetic bilayer, which often causes cell disruption.[18] When lipid membranes are faced with polyelectrolytes, which also contain hydrophobic groups, these are often incorporated into the bilayer instead of self-association.[12] Here, the additional hydrophobic forces were shown to be critical to enable the binding of anionic polymer to neutral and even negatively charged lipid bilayers.[19] Conversely, it was previously shown that excessive polymer hydrophobicity can lead to cell toxicity at a neutral pH value.[20] This is probably caused by the globule configuration adopted by the polymer in the solution. While polyanions seem to be promising materials for intracellular drug delivery, little is known about the potential to manipulate these polymers and they need to be evaluated more carefully.

It was already shown that polyelectrolytes with different polymer backbones (e.g., acrylate, methacrylate, acrylamide, methacrylamide) incorporating large hydrophobic moieties as well as using branched structures increased the interaction with lipid membranes.[21−23] However, to optimize the performance of polyanions and particularly polycarboxylates, their physicochemical properties should be molecularly engineered by the development of tailored, functional polymers with an optimal hydrophilic−lipophilic balance (HLB). Investigations regarding protonation and hydrophobicity of polyanions with tailored structures are needed for the identification of structure−property relationships.

Functional polymers are often prepared from the respective monomers.[24−26] However, if the synthesis of a target polymer to a certain molar mass with narrow dispersity is hampered and/or its corresponding monomer is difficult if not impossible to synthesize, postpolymerization modification (PPM) of reactive prepolymers is the method of choice.[27,28] Some examples are radical thiol−ene,[29] nucleophilic thiol−ene modification,[30] and aminolysis modification with functional polymers.[31,32]

In this context, polymers with activated ester side chains, such as *N*-acryloxysuccinimide (NAS) and pentafluorophenyl acrylate (PFPA), are widely used. Reports have shown that activated ester polymers such as poly(*N*-acryloxysuccinimide) (PNAS) and poly(pentafluorophenyl) acrylate (PPFPA) react fast and quantitively with primary or secondary amines resulting in the corresponding poly(acrylamide) (P(AAm)) derivatives.[33,34] While among activated ester monomers, NAS is the oldest and the most regularly employed one,[35,36] polymers derived from PFPA commonly feature a higher hydrolytic stability and enhanced solubility in a wider range of organic solvents.[34] Previously, PNAS and PPFPA were already employed to synthesize various polymer architectures, such as activated polymer brushes[32,37] and nano(hydro)gels.[38] The modification of activated ester polymers with cross-linking bisamines,[39] amino-modified chromophores,[40,41] amino-sugars,[31] and alkylated amines[42] has been shown. They have further been modified with small peptides.[43−46] However, the modification with amino acids is less explored.

Instead, vinylic polymers with amino acids in the side chains were often retrieved by radical polymerization.[47] Side-chain amino-acid-functionalized poly(meth)acrylates (P(M)A) or poly(meth)acrylamides (P(M)AAm) were obtained from esterified amino acids. The esterification was performed by the Steglich esterification reaction of 2-hydroxyethyl (meth)acrylates or (meth)acrylamides, respectively, with the carboxylic acid moiety of the α-amine-protected amino acid, yielding cationic or zwitterionic polymers.[17,21,48−50] Alternatively, side-chain amino-acid-functionalized P(M)A or P(M)AAm was previously synthesized from the amino-acid-derived vinyl monomers. In general, the monomers were synthesized by the reaction of the carboxylic acid or the amine group of the (protected) amino acid with an activated vinyl compound (e.g., (meth)acryloyl chloride).[3,51,52]

The aim of this study was to synthesize various amino-acid-derived anionic polyacrylamides (P(AA−OH-AAm)) with carboxylic acids in the side chain and tailored hydrophilicity. These polyanions were obtained by the modification of the same PPFPA precursor to obtain fast and quantitative formation of P(AA−OH-AAm). Modification with different amino acids was performed to investigate the correlation between the alkyl side-chain (length and branching) and the physicochemical properties of the polymer. Additionally, we expected the synthesized polyanions to show low-fouling properties due to their peptide-like moieties, enabling applications in the field of protein interactions and delivery materials. Therefore, an investigation was conducted to assess whether different physicochemical properties of the synthesized P(AA−OH-AAm) influence their interactions with proteins and cells to get an initial understanding of their potential applications in a biological environment.

https://doi.org/10.1021/acspolymersau.3c00048
ACS Polym. Au 2024, 4, 222−234

2. RESULTS AND DISCUSSION

2.1. Synthesis and Characterization of Amino-Acid-Derived Polyanions

Neutral α-amino acids with different alkyl substituents in α-position served as starting material for the development of P(AA−OH-AAm) with tailored hydrophilicity. The screened P(AA−OH-AAm) were derived from glycine (Gly), alanine (Ala), aminobutyric acid (Abu), norvaline (Nva), valine (Val), *iso*-leucine (Ile), and leucine (Leu), which were all used in their L-stereospecific form. This library allowed for a comparison of the effect of increasing hydrophobicity (Gly < Ala < Abu < Nva) as well as the effect of side-chain branching (Scheme 1). To ensure high comparability of these polymers and eliminate effects caused by polymer length and dispersity, it was chosen to prepare them via a PPM approach.

Scheme 1. Schematic Representation of the Synthesis of Carboxylated Polyacrylamides with Tailored Hydrophobicity via PPM of PPFPA with Indicated Amino Acids, Yielding Anionic Polymers with Varying Alkyl Substituents[a]

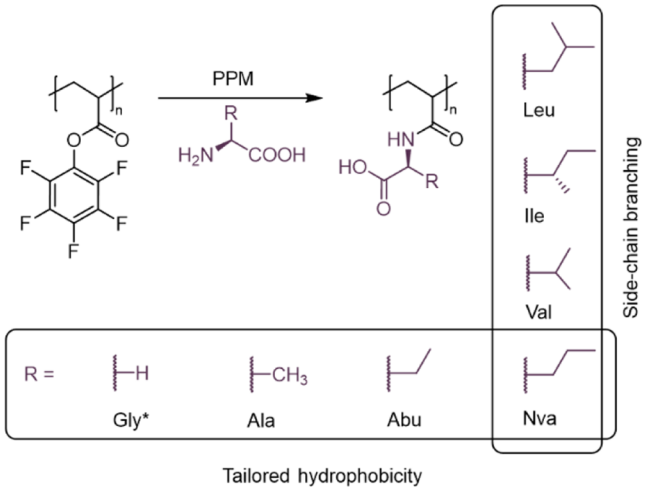

[a]Please note that Gly does not feature a stereo center.

P(AA−OH-AAm) were synthesized by the active ester approach employing the polymerization of PFPA according to Zerdan et al.[53] Reversible addition−fragmentation chain-transfer (RAFT) polymerization proceeded in a controlled manner using a monomer to chain-transfer agent (CTA) ratio of 257 yielding PPFPA ($M_{n,app(PPFPA)}$ = 33,900 g mol^{-1}) with a narrow dispersity ($Đ$ = 1.32) according to size-exclusion chromatography (SEC) measurements (Table 1 and Figure S1). The proton nuclear magnetic resonance (^{1}H NMR) spectrum of PPFPA showed characteristic signals from the backbone protons around δ = 2.0 and 3.0 ppm (Figure 1B).

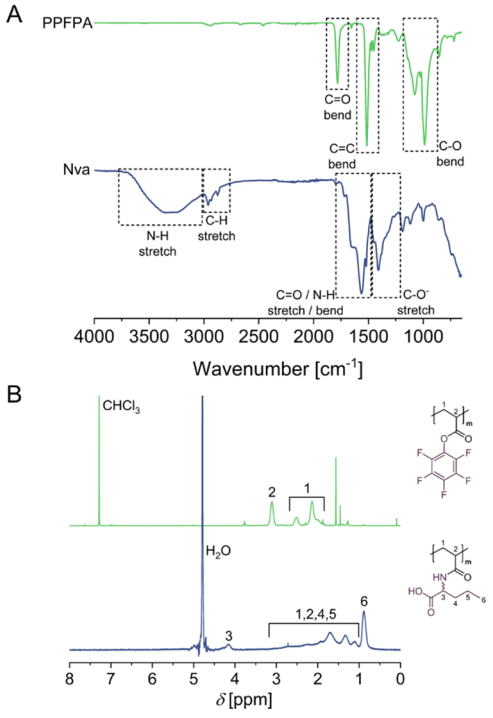

Figure 1. (A) FTIR spectra and (B) ^{1}H NMR spectra (300 MHz) of poly(pentafluorophenyl acrylate) (green, $CDCl_3$) and P(Nva-OH-AAm) (blue, d-DPBS).

Complementary ^{19}F NMR analysis (Figure S2A) showed the expected three signals at δ = −153, − 157, and −163 ppm, which were attributed to the PFP group. The absence of hydrolytic poly(acrylic acid) (PAA) byproducts was confirmed by ^{13}C NMR spectroscopy (Figure S2B). Here, only one type of carbonyl signal was present at δ = 170 ppm, suggesting the absence of hydrolyzed PAA groups in the polymer, which would generally reveal a second carbonyl signal around δ = 180 ppm. In addition, FTIR spectroscopy (Figure S5B) did not show the characteristic PAA band at $\tilde{\nu}$ = 1738 cm^{-1}.[54]

Table 1. Properties of PPFPA and Different Amino-Acid-Functionalized Polymers

polymer name	M^a [g mol^{-1}]	rel. 6-AF by emission[b]	$M_{n,app}{}^c$ [g mol^{-1}]	$Đ^c$	p$K_a{}^d$	ZP[e] [mV]
PPFPA	238.11	n.a.	33,900[f]	1.32[f]	n.a.	n.a.
P(Gly-OH-AAm)	129.12	1.00	11,800	1.73	5.0	−26.6 ± 1.9
P(Ala-OH-AAm)	143.14	1.94	16,300	1.79	5.5	−41.9 ± 1.0
P(Abu−OH-AAm)	157.17	1.06	22,200	1.54	5.1	−37.8 ± 2.3
P(Nva-OH-AAm)	171.2	2.39	13,800	2.77	5.0	−31.1 ± 3.3
P(Val-OH-AAm)	171.2	1.94	22,800	1.43	4.8	−38.4 ± 2.2
P(Ile-OH-AAm)	185.22	1.28	24,900	1.75	5.0	−31.6 ± 1.9
P(Leu-OH-AAm)	185.22	1.23	19,600	1.48	5.1	−37.1 ± 2.2

[a]Molar mass of repeating unit (RU). [b]Fluorescence measurements (λ_{ex} = 450 nm, λ_{em} = 517 nm) in DPBS (1.0 mg mL^{-1}). Values correspond to 6AF-labeled polymers. [c]SEC in 0.07 M aq. Na_2HPO_4 (standard: PMA Na salt). [d]Titration of a 5 mg mL^{-1} polymer solution with 0.1 M HCl. pK_a-value refers to carboxylic acid function. [e]ELS measurements in DPBS (2.0 mg mL^{-1}). [f]SEC in DMAc + 0.21 w% LiCl (standard: PMMA). n.a. not applicable.

https://doi.org/10.1021/acspolymersau.3c00048
ACS Polym. Au 2024, 4, 222−234

PPM of PPFPA was performed by aminolysis with different amino acids comprising varying alkyl substituents in R-position (Scheme 1). A particular challenge was the poor solubility of amino acids in organic solvents.[55,56] Eventually, dimethylformamide (DMF) was chosen as it is regularly employed for PPM of PPFPA,[34] and was found to suspend all amino acids used in this study well. It was further assumed that DMF slightly dissolves amino acids at elevated temperatures.[57] The reaction was performed at 40 °C for 72 h to allow adequate solvation and consumption of the suspended amino acids, leading to a continuous reaction. Hence, PPM of homopolymers with Gly, Ala, Abu, Nva, Val, Ile, and Leu proceeded with the quantitative conversion of the activated ester functional groups yielding the corresponding polyacrylamides P(Gly-OH-AAm), P(Ala-OH-AAm), P(Abu−OH-AAm), P(Nva-OH-AAm), P(Val-OH-AAm), P(Ile-OH-AAm), and P(Leu-OH-AAm), respectively. The success of each synthetic step was verified *via* ^{1}H-, ^{19}F-NMR, and FTIR spectroscopy.

^{1}H NMR spectra of all amino-acid-modified polymers (Figure S3), and exemplarily P(Nva-OH-AAm) in Figure 1B, showed the appearance of a new signal at δ = 4.0 ppm attributed to the C−H adjacent to the newly formed amide bond. Moreover, predominant peaks of CH_3-groups appeared in the spectra ($\delta \approx$ 0.0−2.0 ppm) of amino-acid-derived polymers with long linear alkyl substituents (i.e., Nva) or branched alkyl substituents (i.e., Val, Ile, and Leu). The absence of any peak in ^{19}F NMR spectra (Figure S4) of the AA-side-chain polymer indicated a full conversion of active esters in all PPM reactions.

Additionally, as an example, the FTIR spectra of PPFPA and (P(Nva-OH-AAm) are shown in Figure 1A while the other FTIR spectra are depicted in Figure S5A. Here, the conversion of functional groups is also shown by a shift in absorption band from a carbonyl adjacent to PFPP at $\tilde{\nu}$ = 1780 cm^{-1} to a carbonyl group in an amide bond at $\tilde{\nu}$ = 1550 cm^{-1}.[58] The presence of the carboxylic acid functional group in the polyanions can also be distinguished by its C═O symmetric stretch at $\tilde{\nu}$ = 1410 cm^{-1}. The absence of PAA groups, which may occur as a hydrolytic byproduct, was further suggested by the absence of the characteristic band at $\tilde{\nu}$ = 1738 cm^{-1} (Figure S5B).[54]

SEC measurements (Figure 2 and Table 1) in 0.07 M aqueous Na_2HPO_4 as eluent were performed to verify the integrity of the polymers during the PPM process.

The results revealed an increased $Đ$ (Table 1), potentially related to the more polar eluent and high density of charged groups in the polymers which can cause hydrogen bonding and ionic interactions with the stationary phase leading to broader peaks and longer retention times.[59] Furthermore, the slight high-molar mass shoulder was visible in some polymers, indicating minor chain coupling, which may occur during aminolysis. It was observed that P(AA−OH-AAm) with increasing alkyl chain show shorter elution times (Figure 2A) as can be expected due to the higher molar mass and hydrodynamic volume. Interestingly, branching and the position of branching points also influenced the elution time due to altered sterical hindrance. Figure 2B shows that Val-functionalized polymers (branched alkyl substituent) feature a later elution time, meaning smaller size, compared with Nva-functionalized polymers (linear alkyl substituent). We attribute this apparent smaller size of P(Val-OH-AAm) to their decreased sterical hindrance and more compact alignment of polymers with short-chain branching. A similar trend was

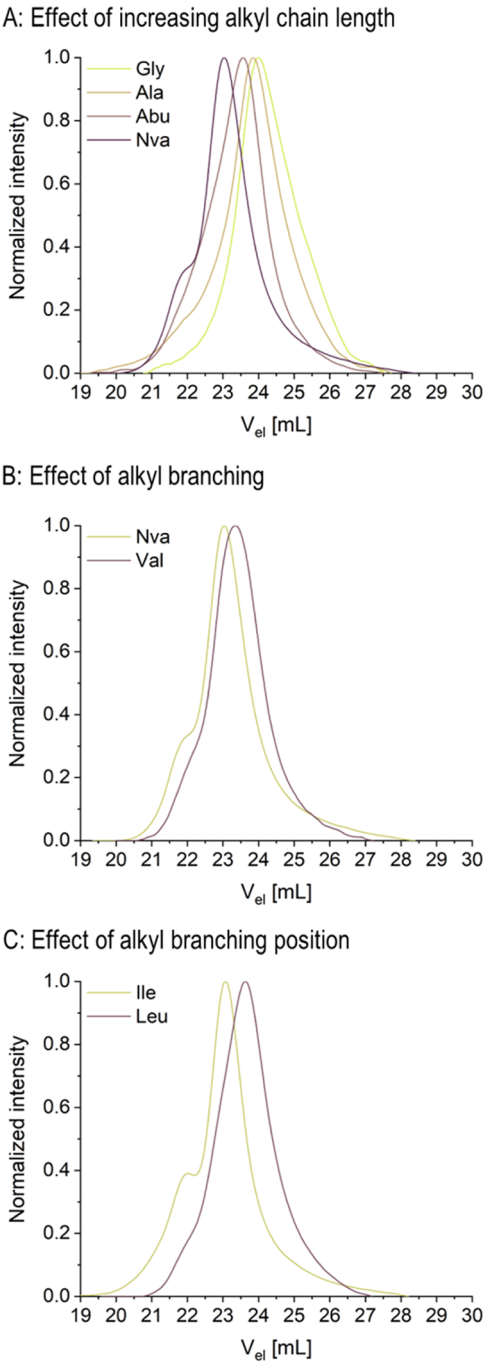

Figure 2. Size-exclusion chromatograms (0.07 M aq. Na_2HPO_4) of P(AA−OH-Aam). (A) Effect of increasing alkyl chain length. (B) Effect of alkyl branching. (C) Effect of alkyl branching position.

observed for polymers modified with P(Ile-OH-AAm) (long-chain branching) and P(Leu-OH-AAm) (terminal short-chain branching) as shown in Figure 2C.

To allow for more in-depth materials characterization as well as biological evaluation, fluorescently labeled P(AA−OH-AAm) were further prepared. Here, a controlled number of fluorescent dye molecules, namely, 6-aminofluorescein (6-AF), was incorporated into the PPFPA prepolymer side chain prior to PPM with amino acids. This method allowed to achieve a similar labeling efficiency of the polymers as was determined by fluorescence spectroscopy measurements (Table 1). The resulting fluorescently labeled P(AA−OH-AAm) will further

https://doi.org/10.1021/acspolymersau.3c00048
ACS Polym. Au 2024, 4, 222−234

be referred to as P(AA−OH-AAm)-6AF. The successful dye labeling was verified by the overlay of SEC traces obtained by the RI and the UV detector (λ = 490 nm; Figure S9). The absence of other signals of the UV trace indicated the absence of unbound dye.

2.2. pH-Responsiveness and Hydrophobicity

Next, the physiochemical properties and *in vitro* properties of the homopolymers were characterized to investigate the influence of the length and branching of alkyl groups in the side chain of polycarboxylates. Acid−base titration was utilized to gain information about the pK_a-values of P(AA−OH-AAm) polymers (Figures S6 and S7). It was found that all P(AA−OH-AAm) possessed pK_a-values between pH = 4.8 and 5.5 attributed to the carboxylic acid in the side chain while some also showed less pronounced pK_a-value around pH ≈ 8, which might be caused by intramolecular interactions with the amide function. The pK_a-values of the carboxylic acids are similar to the pK_a-value of poly(acrylic acid) (pK_a = 4.5).[60] An effect of the alkyl substituent was not observed. ζ Potential measurements of P(AA−OH-AAm) in DPBS (pH = 7.4) verified the presence of a negative surface charge at the physiological pH of the bloodstream (Figure S8A and Table S2). Dynamic light scattering (DLS) measurements in DPBS were performed to exclude aggregation, which could lead to an altered uptake profile. At a polymer concentration of 2 mg mL^{-1}, all P(AA−OH-AAm) revealed a number size distribution of around 10 nm diameter (Figure S8B and Table S1), indicating the absence of larger polymer aggregates in buffered systems.

To assess the extent of influence of the alkyl substituent on the hydrophilicity of P(AA−OH-AAm), high-performance liquid chromatography (HPLC) measurements of all P(AA−OH-AAm)-6AF were performed on a reversed-phase column with an acetonitrile/water gradient. The aqueous phase was acidified with 0.1v% trifluoroacetic acid (TFA) to ensure protonation of the carboxylic acid groups. The polymers showed different retention times related to the hydrophobicity of the alkyl substituent in the side chain (Figure 3A). It was observed that with increasing linear alkyl substituent (Gly < Ala < Abu < Nva), the retention time increased due to the stronger interaction with the column confirming increased hydrophobicity. However, it was also observed that side-chain alkyl branching (i.e., Nva and Val, Ile and Leu) did not affect the hydrophobicity of P(AA−OH-Aam).

These results were further supported by partition coefficient (PC) measurements of P(AA−OH-AAm)-6AF at pH = 7 (Figure 3B), where the decrease of fluorescence of an aqueous polymer solution upon treatment with a hydrophobic $CHCl_3$ phase was quantified by fluorescence spectroscopy measurements. Here, the fluorescence reduction followed the same increasing trend with increasing alkyl chain while revealing similar values for structural isomers. Additionally, the PC of P(AA−OH-AAm) was determined at pH = 4 to gain information about the increase in hydrophobicity at lower pH values. The results in Figure 3B confirmed the expected increased hydrophobicity of carboxylated polymers at pH = 4 compared with pH = 7. In addition, the increase was found to be more drastic for polymers that contained more hydrophobic amino acids in the side chain.

2.3. Protein Fouling of Amino-Acid-Derived Polyanions

To gain important information about the protein fouling of P(AA−OH-AAm), we studied the interaction of two representatives, namely, P(Gly-OH-AAm) and P(Nva-OH-AAm), with bovine serum albumin (BSA) and lysozyme. Here, BSA was chosen as a negatively charged model protein, while lysozyme represented a positively charged model protein.[61] Fouling was analyzed by DLS measurements (Figures 4 and S14 and Table S3), which provided information about the

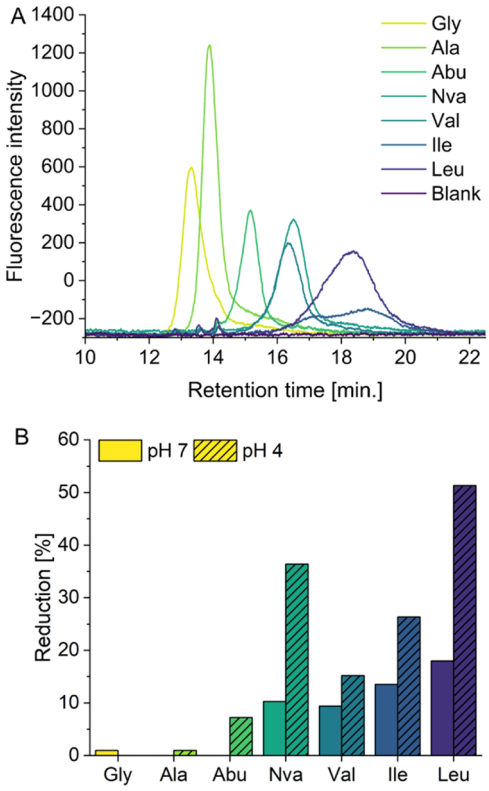

Figure 3. Hydrophilicity of P(AA−OH-AAm). (A) HPLC chromatograms (acetonitrile/water gradient, 0.1v% TFA). Spectra show the absolute fluorescence intensity of eluting 6AF-labeled polymers (λ_{ex} = 480 nm; λ_{em} = 520 nm). (B) pH-dependent relative hydrophilicity of 6AF-labeled polymers. Columns show the reduction of fluorescence of a 0.1 mg mL^{-1} aqueous solution at the indicated pH value after treatment with $CHCl_3$ compared with the fluorescence of the sample prior to treatment with $CHCl_3$. For normalized fluorescence graphs, please refer to Figures S12 and S13.

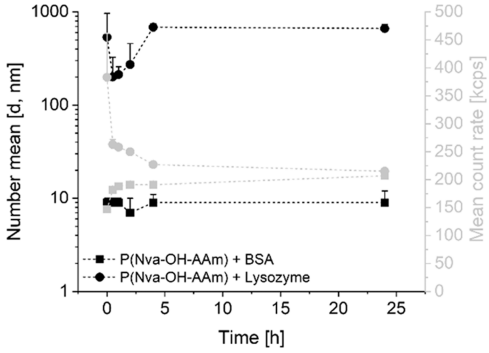

Figure 4. Interaction of P(Nva-OH-AAm) with BSA and Lysozyme. P(Nva-OH-AAm) (c = 0.5 mg mL^{-1}) and indicated proteins (c = 0.5 mg mL^{-1}) were incubated in DPBS at 37 °C for indicated durations. Number mean diameter (black) and mean count rate (gray) were analyzed by DLS measurements at 37 °C. Values (scatter) represent the mean and SD of five measurements with three runs each. Dashed lines do not represent measured values.

https://doi.org/10.1021/acspolymersau.3c00048
ACS Polym. Au 2024, 4, 222−234

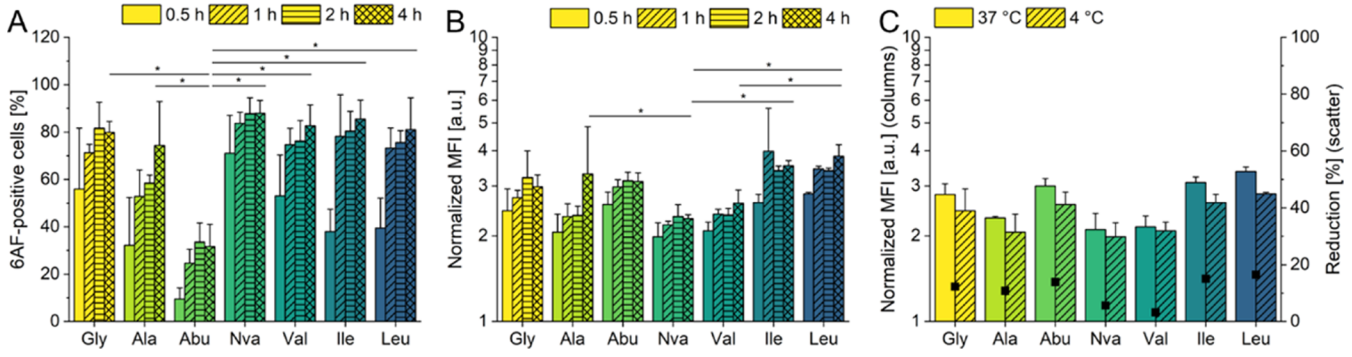

Figure 5. Cellular association of different P(AA−OH-AAm)-6AF determined via flow cytometry measurements. Polymer concentration: 1 mM_{RU}, 50,000 cells seeded in 250 μL in a 48 well plate. Normalized MFI was calculated by eq 3. (A, B) Association of polymers with L929 mouse fibroblasts in DMEM supplemented with 10% FBS. Incubation for indicated time points at 37 °C. (C) Incubation at 37 or 4 °C in DMEM supplemented with 10% FBS for 4 h. Reduction was calculated by eq 4. Statistical analysis (one-way ANOVA with Tukey test) was performed for 4 h incubation time (A, B) to compare the association efficiency of the different P(AA−OH-AAm)-6AF. For temperature-dependent experiments (C), the statistical analysis compared the association at 37 °C versus 4 °C per polymer type. *Indicates a significance of $p < 0.5$. All other comparisons were not statistically significant at $p < 0.5$.

formation of aggregates over time. Owing to the negative charge of P(AA−OH-AAm), a stronger interaction with lysozyme than with BSA was expected. Indeed, mixtures of BSA and P(Nva-OH-AAm) only revealed a minor formation of aggregates, as could be concluded from stable particle diameters and count rates (Figure 4). The aggregation of P(Gly-OH-AAm) with BSA appeared to be slightly increased, which might be caused by increased exposure of the hydrophobic polymer backbone. However, mixtures of P(Nva-OH-AAm) and lysozyme indicated the formation of large nanoparticles ($d \approx 700$ nm) over the course of 4 h, which remained stable up to 24 h. The formation of aggregates was further suggested by a decrease of the mean count rate over time. Lysozyme interacts as well with P(Gly-OH-AAm), leading to, however, smaller aggregates ($d \approx 150$ nm). Thus, the interaction with proteins depends on both, the protein and polymer characteristics, showing stronger interactions with cationic proteins. However, polyanions, in particular sulfated and carboxylated polysaccharides, are known for their good modulation of blood coagulation.[62]

2.4. Interaction of Amino-Acid-Derived Polyanions with Cells

Following the in-depth examination of the obtained polymers, they were tested for their properties in biological systems. As such, the first test should provide information about their cytocompatibility. The cytocompatibility of all P(AA−OH-AAm) was studied by an MTT assay (Figure S15), showing that all polymers were well tolerated by L929 mouse fibroblasts at concentrations up to 0.1 mg mL^{-1} (for 24 h). Additionally, no hemolytic activity at pH 7.4 or 6 and no erythrocyte aggregation were detected at concentrations per repeating unit (c_{RU}) = 1 mM (Figures S16 and S19).

Previously, Duvall and co-workers have screened a library of copolymers with acrylic acid moieties and different hydrophobic alkyl acrylamide units of varying ratios aiming to find an ideal ionic−hydrophobic balance for the modification of cell membranes.[63] Their copolymers further showed some pH-dependent activity. In contrast, the amino-acid-derived anionic polymers of the current study did not reveal any hemolytic activity or erythrocyte aggregation (Figures S16 and S19), emphasizing a favorable balance between anionic character and hydrophobicity. These results further indicated that no membrane disruption and, consequently, no harm to the cells were expected for subsequent cell association experiments.

In previous studies, carboxylated polymers have already shown unique cell association properties. For example, Kempe and co-workers as well as Thayumanavan and colleagues reported the passive diffusion of Cy5-labeled anionic polymers into cells, resulting in mitochondrial colocalization.[7,64] These previous studies also highlighted the importance of the dye for the phenomenon. To avoid passive diffusion, 6AF-labeled polymers were used in the current study. In a preliminary experiment (Figure S20), different concentrations were investigated, in which c_{RU} = 1 mM ($c_{polymer}$ = 4 μM) was determined to be the optimal concentration for subsequent more detailed investigations.

Next, the time-dependent association of polymers with L929 mouse fibroblasts was studied by flow cytometry. It was found that for all seven P(AA−OH-AAm)-6AF, both the mean fluorescence intensity (MFI) and the number of 6AF-positive cells increased over time (Figure 5A,B). Here, polymers with more hydrophobic amino acids (i.e., Nva, Val, Ile, and Leu) showed high cell association with ≥70% 6AF-positive cells after 1 h of incubation. Polymers with more hydrophilic amino acids (i.e., Gly, Ala, and Abu) associated slower to L929 mouse fibroblasts while following an association trend, which is opposite to their hydrophobicity (Gly > Ala > Abu). Based on the results of the protein fouling, one can assume that P(Gly-OH-AAm) revealed some hydrophobic character due to the accessibility of the hydrophobic polymer backbone. Consequently, the polymers follow different association pathways.

Several studies have shown that polymer association or uptake which follows an active pathway, such as endocytosis or macropinocytosis, can be suppressed by lowering the incubation temperature from 37 to 4 °C. Surprisingly, neither the number of 6AF-positive cells nor the MFI dropped significantly when the cells were incubated at a lower temperature (Figure 5C), suggesting the absence of active polymer uptake.

To further investigate the interaction between P(AA−OH-AAm) with cells, L929 fibroblasts were incubated with P(Nva-OH-AAm)-6AF and imaged via confocal laser scanning microscopy (CLSM). We specifically chose this polymer based on its hydrophilic−lipophilic balance (HLB) of 10.05,

https://doi.org/10.1021/acspolymersau.3c00048
ACS Polym. Au 2024, 4, 222−234

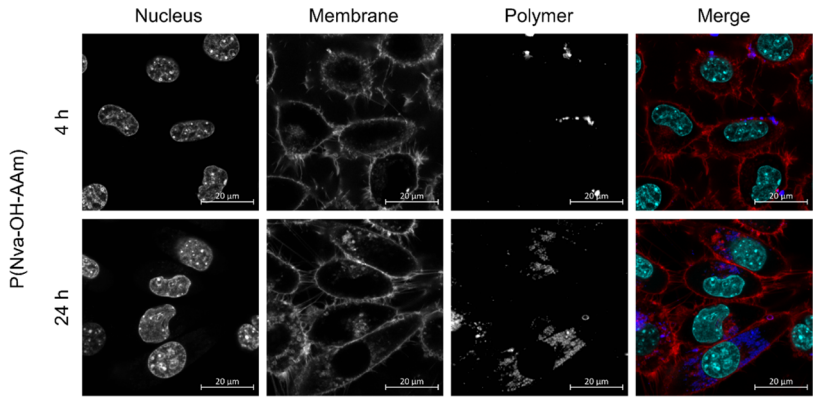

Figure 6. Cellular uptake of P(Nva-OH-AAm)-6AF into L929 mouse fibroblasts visualized by CLSM. Cells were incubated with polymers at 37 °C for indicated times. Cyan: Hoechst 33342/nucleus. Red: CellMask Plasma Membrane Stain/membrane. Blue: 6AF/polymer.

which was calculated after Griffin.[65] In contrast, P(Gly-OH-AAm) possessed an HLB value of 12.83 and could consequently be considered a detergent. A previous study has found that a series of Triton X, commonly applied membrane-permeabilizing agents, possessed altered membrane-disrupting activity depending on their HLB value, which revealed a maximum at an HLB of 12−13 (Triton X-100), while at an HLB of 10, the activity was negligibly low.[66] Other earlier studies have further described the potential to remove phospholipids from cell membranes by anionic detergents such as Triton X-100 or sodium dodecyl sulfate.[67] In particular, the solubilization process relies on the formation of mixed micelles of the detergent and the phospholipids.[68,69] These properties were further suggested after testing the emulsifying properties of P(AA−OH-AAm) with linear alkyl substituents (see the SI for further information).

After 4 h of incubation, a strong colocalization of P(Nva-OH-AAm)-6AF with the cell membrane was observed and no intracellular 6AF signal was detectable (Figure 6). These imaging results provided further clarification on the temperature study as polymer association to cell membranes is mostly a passive process.

To further verify the compatibility and uptake mechanism, L929 mouse fibroblasts were incubated with P(Nva-OH-AAm)-6AF for 24 h. Subsequently, intracellular spot-like fluorescence signals of 6AF were visible, indicating a vesicular localization and, consequently, active albeit very slow polymer internalization. Acute cell death was not observed. Previous studies showed an intracellular mitochondrial colocalization of carboxylated Cy5-labeled polymers after 4 h (passive diffusion).[7] In addition, our previous reports revealed a lysosomal colocalization of glutamic-acid-derived polymers after 4 h (active uptake).[49] However, in the current study, the polymer uptake appeared to be slower compared with these previous reports. In particular, the slow and strong accumulation of anionic polymers at the cell membrane appears to be a rare occurrence in literature. We assume that the combination of anionic and hydrophobic features in our polymers favors this accumulation.

L929 fibroblasts were used as a well-studied eukaryotic model cell line. As such, the cell membrane consists of a phospholipid bilayer, which is characterized by its lipophilic center and anionic outer lipid head groups. Hydrophobic, nonionic polymers are known to interact strongly with these membranes,[70] while anionic polymers generally show very low association.[8] It is assumed that the use of anionic, hydrophobic polymers which may possess both properties leads to the phenomenon of slow membrane integration. In addition, the increasing alkyl chain length inversely correlates with the charge density and, thus, electrostatic repulsion further influencing its accessibility. Therefore, it is important to tune the length of the alkyl chain to find an optimum between hydrophobicity and charge density. Furthermore, we assume that the biomimicking motifs in our amino-acid-derived polymers contributed to the incorporation into the cell membrane. Future studies will focus on a detailed understanding of the cell association of anionic, amino-acid-derived polymers as well as their exploitation for cell-membrane modifications.

3. CONCLUSIONS

P(AA−OH-AAm) with different alkyl substituents were successfully synthesized via PPM of PPFPA which was verified via ^{1}H-, ^{19}F-NMR, and FTIR spectroscopy. Characterization of the physicochemical properties revealed that the alkyl chain did not show any relation between the side chain and the pK_a-value of the carboxylic acid as all were in a similar range of poly(acrylic acid). This emphasizes the complicated nature of the relationship between hydrophobicity and protonation of polyelectrolytes and shows that there are no simple correlations in this complex interplay. ζ-Potential and DLS measurements in DPBS confirmed that the surface charge and no self-assembly occurred. HPLC measurements confirmed the hypothesis that the alkyl chain can tailor the side chain hydrophobicity resulting in increased hydrophobicity for longer alkyl chains. Interestingly, branching in the alkyl chain did not affect the hydrophobicity of P(AA−OH-AAm). The results were supported by PC measurements at pH = 7. Additionally, PC measurement at pH = 4 confirmed the expected increase in hydrophobicity where it was found more drastic for the more hydrophobic P(AA−OH-AAm). All P(AA−OH-AAm) were tolerated by cells up to concentrations of 0.1 mg mL^{-1}. Time-dependent association with L929 fibroblast revealed higher association of more hydrophobic P(AA−OH-AAm), namely, P(Nva-OH-AAm), P(Val-OH-AAm), P(Ile-OH-AAm), and P(Leu-OH-AAm). CLSM measurements revealed that P(Nva-OH-AAm) accumulated at the membrane and was internalized very slowly. Further studies will aim for a more detailed understanding of the cell association of anionic P(AA−OH-AAm) and their molecular engineering to tailor the pH response and membrane interactions further.

https://doi.org/10.1021/acspolymersau.3c00048
ACS Polym. Au 2024, 4, 222−234

4. EXPERIMENTAL PART

4.1. Materials and Instrumentation

4.1.1. Materials. Pentafluorophenyl acrylate (PFPA) was purchased from abcr with 95% purity. 2-(Dodecylthiocarbonothioylthio)-2-methylpropionic acid (DTCTTMPA) (98% purity), Triton X-100, and MEHQ inhibitor remover were purchased from Sigma-Aldrich. The initiator 2,2′-azobis(2,4-dimethylvaleronitril) (V65) was purchased from Wako Chemicals with 98% purity. Acetonitrile was purchased from Fisher Scientific as an extra dry solvent with a purity of 99.9%. THF (stabilized with 0.025% butylated hydroxytoluene) for dialysis was purchased from Fisher Scientific in analytical reagent grade. Dimethylformamide (DMF) was purchased from Fisher Scientific. Amino acids were purchased from Carbolution. 6-Aminofluoresceine (6-AF) was obtained from BLDPharm. Thiazolyl blue tetrazolium bromide (MTT) was obtained from TCI Chemicals. Dulbecco's phosphate buffered saline (DPBS) was purchased from VWR. Dulbecco's Modified Eagle Medium (DMEM) Low Glucose, Fetal Bovine Serum Advanced, Penicillin/Streptomycin (Pen/Strep), and Dulbecco's PBS were purchased from Capricorn Scientific. Polyethylene imine, branched, M_w 10,000 (bPEI 10,000) was purchased from Polysciences Inc. Bovine serum albumin (BSA) and lysozyme were obtained as lyophilized powders from VWR.

4.1.2. Proton Nuclear Resonance (^{1}H NMR) and Fluorine Nuclear Resonance (^{19}F-NMR) Spectroscopy. ^{1}H- and ^{19}F-NMR spectra of PPFPA were recorded on a Bruker Avance Neo Nanobay (300 MHz) spectrometer equipped with a ^{1}H, ^{13}C, ^{19}F, and ^{31}P-BBO probe at room temperature. ^{13}C-NMR spectra of PPFPA were recorded on a Bruker Avance IV (NEO) (500 MHz) spectrometer equipped with a ^{1}H, ^{13}C, and ^{19}F probe at room temperature. Chemical shifts are given in parts per million (ppm or δ-scale) relative to deuterated chloroform or water as indicated in the spectra. Amino-acid-modified polymers were analyzed from deuterated DPBS (d-DPBS), which was prepared by lyophilization of commercial DPBS and subsequent addition of D_2O at an equal volume.

^{1}H- and ^{19}F-NMR spectra of amino-acid-derived polyacrylamides were recorded on a Bruker Avance 300 (300 MHz) spectrometer equipped with a BACS-120 autosampler and a ^{1}H, ^{13}C, ^{19}F, and ^{31}P-BBO probe at room temperature.

4.1.3. Size-Exclusion Chromatography (SEC). SEC measurements of PPFPA were performed on the following setup: Agilent 1200 series, PSS (degasser), G1310A (pump), G1329A (autosampler), Techlab (oven), G7162A (RI detector), G1315D (diode array detector), and PSS GRAM 30 Å guard column and PSS GRAM 1000 Å (10 μm particle size) (column set), dimethylacetamide (DMAc) with 0.21 w% of lithium chloride as additive as eluent at 1 mL min^{-1} at 40 °C, poly(methyl methacrylate) (PMMA) (standard).

Aqueous SEC measurement was performed on an instrument consisting of a column set with a Suprema precolumn (particle size = 5 μm) and three Suprema main columns (particle size = 5 μm, 1 Å × 30 Å; 2 Å × 1000 Å) with separation range from 100 to 1,000,000 Da (PSS, Mainz, Germany) together with a variable wavelength detector (1200 Series, Agilent Technologies). As solvent, 0.07 M aqueous Na_2HPO_4 was used (for dissolving polymer and as eluting solvent) with a flow rate of 0.8 mL min^{-1} and the columns were maintained at room temperature. As internal standard, ethylene glycol (HPLC grade) was used. The calibration was done with narrowly distributed poly(methacrylic acid) sodium salt homopolymers (PMA Na salt; PSS calibration kit). An injection volume of 60 μL was used for the measurements. The samples were dissolved with a concentration of 2 mg mL^{-1} and filtered through a 0.22 μm PTFE Nylon filter before analysis. The UV detector was set to λ = 490 nm for measurements of 6AF-labeled polymers.

Reported molar masses of polymers in this study are based on the indicated standards and denoted as $M_{n,app}$.

4.1.4. High-Performance Liquid Chromatography (HPLC). HPLC measurements were conducted with a Jupiter 5 μm C18 300 Å LC column (250 mm × 4.6 mm). The run time was 35 min. A mixture of 0.1 v/v% TFA in water and acetonitrile served as eluent (Table 2). The fluorescence detected was set to λ_{ex} = 480 nm and λ_{em} = 520 nm with 1× gain. The ELSD detector was set to λ = 215 nm.

Table 2. Composition of HPLC Eluent at Indicated Time Points

time [min]	fraction of 0.1 v/v% aqueous TFA [%]	fraction of acetonitrile [%]
0	98.0	2.0
5	50.0	50.0
10	0.0	100.0
17	0.0	100.0
25	98.0	2.0
35	98.0	2.0

4.1.5. UV-Vis Spectroscopy. Absorption measurements were performed on a Jasco Spectrometer V-670 in the range of 250−500 nm (scan speed 400 nm min^{-1}) at 25 °C using a quartz glass cuvette (D = 10 mm). Baseline correction was carried out by measuring a blank sample with deionized water before measurements.

4.1.6. Fluorescence Spectroscopy. Fluorescence emission (λ_{em} = 517 nm) curves were measured on a Shimadzu RF 5301 PC spectro-fluorophotometer at an excitation wavelength of 450 nm using a quartz glass cuvette (D = 10 mm). Baseline correction was carried out by a background measurement prior to the sample measurement.

4.1.7. Dynamic Light Scattering (DLS). DLS was measured on a Zetasizer Nano-ZS Malvern apparatus (Malvern Instruments Ltd.) using disposable cuvettes. The excitation light source was a He−Ne laser at 633 nm and the intensity of the scattered light was measured at an angle of 173°. This method measures the rate of intensity fluctuation, and the size of the particles is determined through the Stokes−Einstein equation. Results are based on the material's properties of polystyrene latexes through the settings of the instrument. The concentration of the polymer solution was 2 mg mL^{-1} (in DPBS) in all cases. Details regarding size results as well as count rates can be found in Table S1.

4.1.8. Electrophoretic Light Scattering (ELS). ELS was used to measure the zeta potential (ζ). The measurement was also performed on a Zetasizer Nano-ZS by applying laser Doppler velocimetry. For each measurement, 20 runs were carried out using the slow-field reversal and the fast-field reversal mode at 150 V. Each experiment was performed in triplicates at 25 °C. The zeta potential was calculated from the electrophoretic mobility (μ) according to the Henry equation. Henry coefficient f(ka) was calculated according to Ohshima.[71] The concentration of the polymer solution was 2 mg mL^{-1} (in DPBS) in all cases. Details regarding charge results as well as count rates can be found in Table S2.

4.1.9. Fourier-Transform Infrared Spectroscopy (FTIR). IR spectra were recorded from solids on a PerkinElmer Spectrum 100 FTIR spectrometer in attenuated total reflection (ATR) mode.

4.2. Synthesis and Characterization

4.2.1. Poly(pentafluorophenyl) Acrylate (PPFPA). Poly(pentafluorophenyl) acrylate was prepared utilizing a modified procedure originally described by Zerdan et al.[53]

Ten grams of pentafluorophenyl acrylate (PFPA) was transferred into a 10 mL vial and stirred with inhibitor remover for 49 min. Meanwhile, a 25 mL round-bottom flask equipped with a rare earth stirring bar was heated with a heat gun. The atmosphere inside the flask was converted into an argon atmosphere by three cycles of applying a vacuum and subsequently filling the flask with argon. Afterward,12 mL (9.4 g) of anhydrous acetonitrile was transferred to the flask. 55 mg (0.151 mmol) of the chain-transfer agent (CTA) 2-(dodecylthiocarbonothyolthio)-2-methylpropionic acid (DTCTTMPA) was added to the reaction flask and the solution was stirred until all DTCTTMPA was dissolved. Afterward, the monomer was separated from the inhibitor remover utilizing a needle with a smaller diameter than the diameter of the inhibitor remover

https://doi.org/10.1021/acspolymersau.3c00048
ACS Polym. Au 2024, 4, 222−234

beads. 9.21 g (38.69 mmol) of the monomer PFPA was added to the flask to achieve a ratio of monomer:CTA of 257:1. A solution of V65 in acetonitrile (c = 10 mg mL^{-1}) was then prepared and 937 μL (0.038 mmol) of the solution was added to the flask and it was sealed with a rubber septum. The final monomer:CTA:initiator ratio was 257:1:0.25. The mixture was stirred for 2 min to homogenize the solution before it was purged with argon for 15 min. The yellow mixture was then transferred into a preheated oil bath thermostated at 60 °C and stirred for 17 h. The mixture was subsequently transferred to a dialysis tubing (Spectrum Spectra/Por Cellulose Ester, MWCO: 8 kDa), and dialysis against THF was performed for 3 days with daily solvent change. Then, the solvent was removed under reduced pressure and the polymer was dried in a vacuum oven at 60 °C for 1 day. The product was obtained as a yellow solid. Yield: 1.97 g (21%).

The DP of the resulting polymer was calculated by end-group analysis, using the signal of the CTA's terminal CH_3 group at δ = 0.91 ppm and the CH group of the polymer backbone at δ = 3.12 ppm, suggesting a DP of 132.

SEC (DMAc + 0.21 w% LiCl; PMMA-standard): $M_{n,app}$ = 33,900 g mol^{-1}; $Đ$ = 1.32.

4.2.2. Postpolymerization Modification of PPFPA with Aliphatic Amino Acids. The postpolymerization modification of PPFPA is exemplarily described for reactions with Gly-yielding P(Gly-OH-AAm). Quantities and moles are given relative to the single repeating unit PFPA of the polymer and can be found in Table 3.

Table 3. Quantities of Amino Acids Used for PPM of PPFPA

amino acid	n [mmol]	m [mg]
Gly	1.26	95
Ala		112
Abu		130
Nva		148
Val		148
Ile		165
Leu		165

In a 5 mL reaction vessel (Biotage), PPFPA (100 mg, 0.42 mmol, 1.00 equiv) was dissolved in anhydrous DMF (5 mL). 250 μL of triethylamine was added. After that, Gly (95 mg, 1.26 mmol, 3 equiv) was added, the reaction vial was closed with a septum, and the suspension was stirred at 40 °C for 72 h. Then, the solid was filtered off and the remaining solution was dialyzed (RC, MWCO 3.5 kDa, SpectraPor) against 1 L of deionized water for 3 days with daily water change. Upon lyophilization, the product was yielded as an off-white to yellowish powder. Polymers were analyzed via ^{1}H NMR, ^{19}F-NMR, FTIR spectroscopy, and aqueous SEC. ^{1}H NMR showing C−H adjacent to an amide bond (δ = 4.0 ppm) and FTIR showing a shift in absorption from a carbonyl adjacent to PFP at $\tilde{\nu}$ = 1780 cm^{-1} toward a carbonyl group in an amide bond $\tilde{\nu}$ = 1550 cm^{-1} both confirmed the conversion of the reaction. NMR and FTIR spectra can be found in the Supporting Information. Molar mass and dispersity from SEC measurements can be found in Table 1.

4.2.3. Postpolymerization Modification of PPFPA with 6-AF and Aliphatic Amino Acids. The postpolymerization modification of PPFPA is exemplarily described for reactions with Gly-yielding P(Gly-OH-AAm)-6AF. Quantities and moles are given relative to the single repeating unit PFPA of the polymer and can be found in Table 3.

In a 5 mL reaction vessel (Biotage), PPFPA (100 mg, 0.42 mmol, 1.00 equiv) was dissolved in anhydrous DMF (5 mL). Twenty-five μL triethylamine was added. After that, 6-AF (1 mg, 0.004 mmol, 0.01 equiv) was added and the reaction vessel was closed with a septum. The reaction mixture was stirred in the dark at 40 °C for 24 h. Then, 225 μL of triethylamine and Gly (95 mg, 1.26 mmol, 3 equiv) were added, the reaction vial was closed with a septum, and the suspension was stirred at 40 °C for 72 h. Then, the solid was filtered off and the remaining solution was dialyzed (RC, MWCO 3.5 kDa, SpectraPor) against 1 L of deionized water for 3 days with daily water changes. Upon lyophilization, the product was yielded as a yellow to greenish powder. Yields were determined gravimetrically. The labeling efficiency (LE) was determined by UV−vis measurements in DPBS according to the calibration of pure 6-AF in DPBS (Figure S10).

Yields (% assuming quantitative amino acid modification) and LE:
P(Gly-OH-AAm)-6AF: 19 mg (35%); LE: 11%
P(Ala-OH-AAm)-6AF: 48 mg (80%); LE: 14%
P(Abu−OH-AAm)-6AF: 47 mg (71%); LE: 8%
P(Nva-OH-AAm)-6AF: 45 mg (63%); LE: 12%
P(Val-OH-AAm)-6AF: 45 mg (63%); LE: 13%
P(Ile-OH-AAm)-6AF: 48 mg (62%); LE: 10%
P(Leu-OH-AAm)-6AF: 52 mg (67%); LE 9%

Polymers were analyzed by aqueous SEC (0.07 M aq. Na_2HPO_4 (standard: PMA Na salt)). Elugrams can be found in Figure S9.
P(Gly-OH-AAm)-6AF: $M_{n,app}$ = 11,500 g mol^{-1}; $Đ$ = 1.84.
P(Ala-OH-AAm)-6AF: $M_{n,app}$ = 14,200 g mol^{-1}; $Đ$ = 1.70.
P(Abu−OH-AAm)-6AF: $M_{n,app}$ = 13,800 g mol^{-1}; $Đ$ = 1.70.
P(Nva-OH-AAm)-6AF: $M_{n,app}$ = 13,400 g mol^{-1}; $Đ$ = 1.62.
P(Val-OH-AAm)-6AF: $M_{n,app}$ = 14,200 g mol^{-1}; $Đ$ = 1.57.
P(Ile-OH-AAm)-6AF: $M_{n,app}$ = 16,300 g mol^{-1}; $Đ$ = 1.55.
P(Leu-OH-AAm)-6AF: $M_{n,app}$ = 10,500 g mol^{-1}; $Đ$ = 2.11.

4.2.4. pH Response. The pH response of the different polymers was investigated by acidic titration. A 5 mg mL^{-1} solution of the polymer in deionized water was prepared and 20 μL of 1.0 M aq. NaOH was added to obtain a starting pH value >11. Subsequently, the solution was titrated with 0.1 M aq. HCl until a pH value <3 was reached. Measurements were done with a Mettler Toledo digital pH meter. The pK_a was calculated from the first derivation of the titration curve according to our previous work.[72]

4.2.5. Hydrophilic/Hydrophobic Ratio. The procedure was modified from the literature.[21] A known concentration of amino-acid-functionalized polymers (1 or 0.1 mg mL^{-1} as indicated) was dissolved in deionized water (diH_2O) of indicated pH value or DPBS. To ensure precise pH values, 200 μL of a 10-fold stock solution of the respective polymer was diluted with diH_2O to a total volume of 1.5 mL. The pH value was adjusted by the addition of an aqueous 0.1 M HCl or NaOH solution. After the desired pH value was reached, diH_2O was added to reach a final volume of 2.0 mL. The fluorescence of this solution was measured. Then, an equal volume of chloroform was added, and the solution was vortexed for 1 min at maximum speed. The 0.1 mg mL^{-1} solution was allowed to stand for 15 min (or 24 h in the case of 1 mg mL^{-1} solutions) to separate the aqueous and the organic layer. A sample was carefully taken from each layer and analyzed via fluorescence measurements (λ_{ex} = 450 nm, λ_{em} = 517 nm). To obtain the relative fluorescence, the raw results were normalized by the peak maximum of the emission trace of the respective polymer observed before the addition of chloroform (eq 1). The results show the normalized fluorescence intensity.

$$\text{relative fluorescence emission} = \frac{\text{intensity after chloroform treatment}}{\text{intensity before chloroform treatment}} \quad (1)$$

The hydrophobic−lipophilic balance (HLB) of polymers was predicted with MarvinSketch 23.14 using the Griffin method.[65]

4.2.6. Protein Fouling. Protein fouling of P(Gly-OH-AAm) and P(Nva-OH-AAm) with BSA and lysozyme, respectively, was analyzed by DLS measurements.

Stock solutions of the polymers and the proteins in DPBS were prepared (c = 1 mg mL^{-1}) and mixed in a ratio of 1:1, yielding concentrations of c = 0.5 mg mL^{-1}. The samples were measured immediately after mixing (t = 0 h) and at indicated time points (i.e., 0.5, 1, 2, 4, and 24 h). The time points indicate the time interval in-between measurements at which the samples were incubated at 37 °C while shaking at 100 rpm. Measurements were conducted at 37 °C with five measurements and three runs each. After the measurement, samples were placed back into the incubator immediately.

4.2.7. Statistical Analysis. All data plotted with error bars were expressed as means with standard deviation. p-Values were generated

https://doi.org/10.1021/acspolymersau.3c00048
ACS Polym. Au 2024, 4, 222−234

by analyzing data with a one-way ANOVA and Turkey test using OriginLab.

4.3. Biological Evaluation

4.3.1. Cell Culture. L929 cells were cultured in low-glucose Dulbecco's Modified Eagle Medium (DMEM) supplemented with 10% fetal bovine serum, 100 U mL^{-1} penicillin, and 100 μg mL^{-1} streptomycin. The cells were incubated at 37 °C using 5% CO_2 in a humidified incubator.

4.3.2. Cell Viability Assay. The cell viability assay was slightly modified from our previous procedure.[2] Cells were cultured as described above. For the cell viability assay, cells (10^4 per well) were seeded in 96 well plates and allowed to adhere overnight. No cells were seeded in the outer wells. The media was subsequently removed and replaced by fresh polymer-containing media. Then, the cells were incubated at 37 °C for an additional 24 h. After that, the media was removed, the cells were washed with 100 μL of DPBS, and then fresh media containing thiazolyl blue tetrazolium bromide (MTT) (concentration: 1 mg mL^{-1}) was added (100 μL/well). Note: MTT (50 mg) was dissolved in 10 mL of sterile PBS, filtrated (membrane, 0.22 μm), and 1 to 5 diluted in culture medium prior to use in this assay. After incubation for 3 h at 37 °C, 100 μL of *i*-PrOH was added to each well and the plates were gently shaken in the dark for 15 min to dissolve the formazan crystals. Quantification was done by measuring the absorbance at λ = 580 nm using a microplate reader (Genios Pro, Tecan). Untreated cells on the same plate served as negative control (100% viability), cells treated with 20% DMSO as positive control (0% viability), and wells without cells as background. Experiments were formed in triplicates on three different plates. Relative cell viability was calculated by using eq 2.

$$\%\ \text{cell viability} = \frac{\text{Abs. sample} - \text{Abs. background}}{\text{Abs. negative control} - \text{Abs. background}} \times 100 \quad (2)$$

4.3.3. Cell Association via Flow Cytometry. *4.3.3.1. Cell Association Assay I: Concentration-Dependent Polymer Association with L929.* The cell association assay is adapted from Leiske et al.[21] The L929 cells were cultured at 37 °C in a humidified 5% (v/v) CO_2 atmosphere in DMEM Low Glucose (1 g L^{-1}). The media was supplemented with 10% (v/v) fetal bovine serum (FBS), 100 U mL^{-1} penicillin, and 100 μg mL^{-1} streptomycin (culture medium). For the experiments, 2×10^5 cells mL^{-1} were seeded in 250 μL of culture medium in a 48 well plate and cultivated for 24 h until treatment. One hour before the treatment, the medium was changed to 225 μL of fresh culture medium. The polymers were diluted in DPBS to a concentration of c_{RU} = 0.5, 1.0, 5.0, and 10 mM. Cells were treated with 25 μL of respective polymer to receive final concentrations of c_{RU} = 0.05, 0.10, 0.50, and 1.00 mM. Cells were additionally treated with 25 μL of DPBS as negative control (NC). After 4 h of incubation at 37 °C, 5% (v/v) CO_2, the supernatant was discarded. The cells were immediately detached with trypsin-EDTA, resuspended in PBS, and analyzed by flow cytometry (cytoFLEX (Beckman Coulter)). A minimum of 10,000 single cells were measured and analyzed by forward and sideward scatter (FSC/SSC). Fluorescence was measured at λ_{ex} = 488 nm with a 510/20 nm bandpass filter (GFP channel). Positive cells were identified by gating against NC. A detailed gating strategy is provided in Figure S17.

The normalized MFI was calculated using eq 3.

$$\text{normalized MFI[a. u.]} = \frac{\text{MFI}_{\text{sample}}}{\text{MFI}_{\text{NC}}} \times \frac{1}{r\ \text{fluorescence}_{\text{sample}}} \quad (3)$$

4.3.3.2. Cell Association Assay II: Time- and Temperature-Dependent Polymer Association with L929. L929 cells were seeded as described before and cultivated for 24 h until treatment. One hour before the treatment, the medium got changed to 225 μL of fresh culture medium. The polymers were diluted in DPBS to a concentration of c_{RU} = 10 mM. Cells were treated with 25 μL of the respective polymer at different time points to achieve final incubation times of 0.5, 1.0, 2.0, and 4.0 h at 37 °C, 5% (v/v) CO_2 with c_{RU} = 1.0 mM. Cells were additionally treated with 25 μL of DPBS as NC. An additional 48 well plate was treated in parallel at 4 °C (refrigerator) for 4 h. After incubation, the cells were measured as described before. A detailed gating strategy is provided in Figure S18.

The normalized MFI was calculated using eq 3. The temperature-dependent reduction of cell association was calculated using eq 4.

$$\text{reduction}[\%] = 1 - \frac{\text{MFI}_{4^\circ\text{C}}(\text{normalized})}{\text{MFI}_{37^\circ\text{C}}(\text{normalized})} \times 100\% \quad (4)$$

4.3.4. Confocal Laser-Scanning Microscopy (CLSM). The assay is adapted from Richter et al.[73] For cell association studies, cells were seeded as described before in 500 μL of culture medium in 4 well glass-bottomed dishes (Greiner Bio-One, Cat# 627860) and cultivated for 24 h until treatment. One hour prior to treatment, the medium got changed to 450 μL of fresh culture medium. The polymers were diluted in DPBS to a concentration of 10 mM (RU). Cells were treated with 50 μL of the polymer to achieve a final concentration of 1.0 mM (RU) and incubated for 4 or 24 h at 37 °C in humidified 5% (v/v) CO_2. To stain nuclei, Hoechst 33342 (Invitrogen, Cat# H3570) was added (1:1000). To stain cellular membrane, CellMask Plasma Membrane Stain (Invitrogen, Cat# C10046) was added (1:1000). After further incubation of 10 min, the medium was replaced by 500 μL of fresh medium. Live cell imaging was performed using a LSM880, Elyra PS.1 system (Zeiss) applying laser for excitation at 405 nm (1.0%) (emission filter 410−484 nm, detection of Hoechst), 488 nm (2.0%) (emission filter 490−579 nm, detection of fluorescein), and 633 nm (1.5%) (emission filter 638−759 nm, detection of CellMask). To avoid cross-talk between the dyes, three different tracks were used. Images were acquired using the ZEN software, version 2.3 SP1 (Zeiss). The experiments were performed at least twice. All images were processed with ZEN software, version 3.7 (ZEN lite) (Zeiss). The same values were applied to all images.

4.3.5. Hemoglobin Release and Erythrocyte Aggregation. The erythrocyte aggregation and hemoglobin release assay were adapted from Richter et al.[73] The interaction of polymers with cellular membranes was detected by measuring the release of hemoglobin from erythrocytes due to potential membrane lysis. The blood, collected in tubes with citrate, was provided by the Department of Transfusion Medicine of the University Hospital, Jena. The experimental protocols used therein were approved by the ethics committee of the Jena University Hospital (2021−2058-Material). Blood from at least three different human donors was used. To isolate erythrocytes, the blood was centrifuged at 4500*g* for 5 min. The pellet was washed three times with DPBS. 500 μL of aliquots of erythrocytes were mixed with 500 μL of polymer solution in DPBS to receive a final concentration of c_{RU} = 1 mM (Test solution). To determine aggregation, 100 μL of the respective test solutions were transferred to a 96 well plate in three technical replicates. bPEI 10000 was used as a positive control (50 μg mL^{-1}) and only DPBS as NC. After incubation at 37 °C for 2 h, the absorbance was measured at λ = 645 nm. The aggregation rate was calculated by eq 5.

$$\text{aggregation rate} = \frac{\text{absorbance}_{\text{NC}}}{\text{absorbance}_{\text{sample}}} \quad (5)$$

Exemplary microscopy images of aggregation are provided in Figure S19.

In parallel, the remaining 700 μL of test solutions was incubated for 1 h at 37 °C. To determine hemoglobin release, the tubes were centrifuged at 2400*g* for 5 min and the supernatant was transferred to a 96 well plate in three technical replicates. To measure the hemolytic effect of the polymers, the absorbance was measured at λ = 544 with λ = 630 nm as reference bandwidth. As a positive control, 1% Triton X-100 (T-X) was used (100% hemolysis) and pure DPBS was used as NC. The hemolysis (%) was calculated using eq 6.

https://doi.org/10.1021/acspolymersau.3c00048
ACS Polym. Au 2024, 4, 222−234

$$\text{hemolysis}(\%) = \frac{\text{absorbance}_{\text{sample}}}{\text{absorbance}_{\text{T-X}}} \times 100 \quad (6)$$

Values below 2% hemolysis are classified as nonhemolytic, values between 2 and 5% are slightly hemolytic, and values above 5% are hemolytic.

■ ASSOCIATED CONTENT

Supporting Information

The Supporting Information is available free of charge at https://pubs.acs.org/doi/10.1021/acspolymersau.3c00048.

The Supporting Information is available free of charge and contains further analysis of the materials in this study, including ^{1}H and ^{19}F-NMR spectra, fluorescence spectra, FTIR spectra, SEC data, cell viability data, cell association, and uptake data (PDF)

■ AUTHOR INFORMATION

Corresponding Author

Meike N. Leiske − *Macromolecular Chemistry, University of Bayreuth, 95447 Bayreuth, Germany; Bavarian Polymer Institute, 95447 Bayreuth, Germany;* orcid.org/0000-0002-8525-2324; Email: meike.leiske@uni-bayreuth.de

Authors

Jonas De Breuck − *Macromolecular Chemistry, University of Bayreuth, 95447 Bayreuth, Germany*

Michael Streiber − *Laboratory of Organic and Macromolecular Chemistry (IOMC), Friedrich Schiller University Jena, 07743 Jena, Germany; Jena Center for Soft Matter (JCSM), Friedrich Schiller University Jena, 07743 Jena, Germany*

Michael Ringleb − *Laboratory of Organic and Macromolecular Chemistry (IOMC), Friedrich Schiller University Jena, 07743 Jena, Germany; Jena Center for Soft Matter (JCSM), Friedrich Schiller University Jena, 07743 Jena, Germany;* orcid.org/0000-0002-7320-8529

Dennis Schröder − *Macromolecular Chemistry, University of Bayreuth, 95447 Bayreuth, Germany; Bavarian Polymer Institute, 95447 Bayreuth, Germany*

Natascha Herzog − *Macromolecular Chemistry, University of Bayreuth, 95447 Bayreuth, Germany*

Ulrich S. Schubert − *Laboratory of Organic and Macromolecular Chemistry (IOMC), Friedrich Schiller University Jena, 07743 Jena, Germany; Jena Center for Soft Matter (JCSM), Friedrich Schiller University Jena, 07743 Jena, Germany;* orcid.org/0000-0003-4978-4670

Stefan Zechel − *Laboratory of Organic and Macromolecular Chemistry (IOMC), Friedrich Schiller University Jena, 07743 Jena, Germany; Jena Center for Soft Matter (JCSM), Friedrich Schiller University Jena, 07743 Jena, Germany*

Anja Traeger − *Laboratory of Organic and Macromolecular Chemistry (IOMC), Friedrich Schiller University Jena, 07743 Jena, Germany; Jena Center for Soft Matter (JCSM), Friedrich Schiller University Jena, 07743 Jena, Germany;* orcid.org/0000-0001-7734-2293

Complete contact information is available at: https://pubs.acs.org/10.1021/acspolymersau.3c00048

Author Contributions

[⊥]M.S. and M.R. contributed equally to this work. The primary data are available. CRediT: **Jonas De Breuck** data curation, formal analysis, methodology, writing-original draft; **Michael Streiber** data curation, formal analysis, methodology, writing-review & editing; **Michael Ringleb** data curation, formal analysis, methodology, writing-review & editing; **Dennis Schröder** data curation, formal analysis, writing-review & editing; **Natascha Herzog** data curation, formal analysis; **Ulrich S. Schubert** funding acquisition, supervision, writing-review & editing; **Stefan Zechel** project administration, supervision, writing-review & editing; **Anja Traeger** conceptualization, funding acquisition, project administration, supervision, writing-review & editing; **Meike N. Leiske** conceptualization, funding acquisition, supervision, writing-original draft.

Notes

The authors declare no competing financial interest.

■ ACKNOWLEDGMENTS

The authors would like to acknowledge Prof Ruth Freitag, Prof Andreas Greiner, Prof Hans-Werner Schmidt, Prof Thomas Scheibel, and Prof Georg Papastavrou for providing access to their laboratories and equipment. The authors thank Dr Martin Humenik for his help with high-performance liquid chromatography measurements. The authors would like to thank Rika Schneider for conducting size-exclusion chromatography measurements, Martina Fried for assistance with polymer titrations, and Carolin Kellner for support with hemolysis and erythrocyte aggregation assays. M.N.L. acknowledges the financial support from the "Fonds der Chemischen Industrie im Verband der Chemischen Industrie." The authors gratefully acknowledge the Bundesministerium für Bildung und Forschung (BMBF, Germany, #13XP5034A PolyBioMik), the DFG Projects PolyTarget (SFB 1278, project B01, C06, project ID: 316213987) as well as the "Thüringer Aufbaubank (TAB)" (2021 FGI 0005), and the "Europäischer Fond für regionale Entwicklung (EFRE)" (2018FGI0025) for funding of flow cytometry devices at the Jena Center for Soft Matter (JCSM). This work was performed within the Joint Lab for Polymers Jena-Bayreuth.

■ REFERENCES

(1) Duncan, R.; Gaspar, R. Nanomedicine(s) under the Microscope. *Mol. Pharmaceutics* **2011**, *8* (6), 2101−2141.

(2) Villaverde, G.; Baeza, A. Targeting Strategies for Improving the Efficacy of Nanomedicine in Oncology. *Beilstein J. Nanotechnol.* **2019**, *10*, 168−181.

(3) Takano, S.; Sakurai, K.; Fujii, S. Internalization into Cancer Cells of Zwitterionic Amino Acid Polymers via Amino Acid Transporter Recognition. *Polym. Chem.* **2021**, *12* (42), 6083−6087.

(4) Li, Y.; Yang, H. Y.; Thambi, T.; Park, J. H.; Lee, D. S. Charge-Convertible Polymers for Improved Tumor Targeting and Enhanced Therapy. *Biomaterials* **2019**, *217*, No. 119299, DOI: 10.1016/j.biomaterials.2019.119299.

(5) Choi, H. S.; Liu, W.; Liu, F.; Nasr, K.; Misra, P.; Bawendi, M. G.; Frangioni, J. V. Design Considerations for Tumour-Targeted Nanoparticles. *Nat. Nanotechnol.* **2010**, *5* (1), 42−47.

(6) Theodorou, I.; Anilkumar, P.; Lelandais, B.; Clarisse, D.; Doerflinger, A.; Gravel, E.; Ducongé, F.; Doris, E. Stable and Compact Zwitterionic Polydiacetylene Micelles with Tumor-Targeting Properties. *Chem. Commun.* **2015**, *51* (80), 14937−14940.

(7) Mahmoud, A. M.; de Jongh, P. A. J. M.; Briere, S.; Chen, M.; Nowell, C. J.; Johnston, A. P. R.; Davis, T. P.; Haddleton, D. M.; Kempe, K. Carboxylated Cy5-Labeled Comb Polymers Passively Diffuse the Cell Membrane and Target Mitochondria. *ACS Appl. Mater. Interfaces* **2019**, *11* (34), 31302−31310.

(8) Wang, S. PH-Responsive Amphiphilic Carboxylate Polymers: Design and Potential for Endosomal Escape. *Front. Chem.* **2021**, *9* (March), 1−8.
(9) Li, M.; Zhang, W.; Li, J.; Qi, Y.; Peng, C.; Wang, N.; Fan, H.; Li, Y. Zwitterionic Polymers: Addressing the Barriers for Drug Delivery. *Chin. Chem. Lett.* **2023**, *34* (11), No. 108177.
(10) Monnery, B. D. Polycation-Mediated Transfection: Mechanisms of Internalization and Intracellular Trafficking. *Biomacromolecules* **2021**, *22* (10), 4060−4083.
(11) Agarwal, S.; Zhang, Y.; Maji, S.; Greiner, A. PDMAEMA Based Gene Delivery Materials. *Mater. Today* **2012**, *15* (9), 388−393.
(12) Yessine, M. Membrane-Destabilizing Polyanions: Interaction with Lipid Bilayers and Endosomal Escape of Biomacromolecules. *Adv. Drug Delivery Rev.* **2004**, *56* (7), 999−1021.
(13) Behr, J.-P. The Proton Sponge: A Trick to Enter Cells the Viruses Did Not Exploit. *Chimia Aarau* **1997**, *51* (1−2), 34.
(14) Bus, T.; Traeger, A.; Schubert, U. S. The Great Escape: How Cationic Polyplexes Overcome the Endosomal Barrier. *J. Mater. Chem. B* **2018**, *6* (43), 6904−6918.
(15) Braksch, C. P.; Lehnen, A. C.; Bapolisi, A. M.; Gurke, J.; De Breuck, J.; Leiske, M. N.; Hartlieb, M. Staphylococcus Aureus Selective Antimicrobial Polymers Based on an Arginine-Derived Monomer. *J. Polym. Sci.* **2024**, *62* (1), 132−145.
(16) Lehnen, A. C.; Kogikoski, S.; Stensitzki, T.; AlSawaf, A.; Bapolisi, A. M.; Wolff, M.; De Breuck, J.; Müller-Werkmeister, H. M.; Chiantia, S.; Bald, I.; Leiske, M. N.; Hartlieb, M. Anisotropy in Antimicrobial Bottle Brush Copolymers and Its Influence on Biological Activity. *Adv. Funct. Mater.* **2023**, No. 2312651, DOI: 10.1002/adfm.202312651.
(17) Nayak, K.; Ghosh, P.; Khan, M. E. H.; De, P. Side-Chain Amino-Acid-Based Polymers: Self-Assembly and Bioapplications. *Polym. Int.* **2022**, *71* (4), 411−425.
(18) Kauffman, W. B.; Fuselier, T.; He, J.; Wimley, W. C. Mechanism Matters: A Taxonomy of Cell Penetrating Peptides. *Trends Biochem. Sci.* **2015**, *40* (12), 749−764.
(19) Ladavière, C.; Toustou, M.; Gulik-Krzywicki, T.; Tribet, C. Slow Reorganization of Small Phosphatidylcholine Vesicles upon Adsorption of Amphiphilic Polymers. *J. Colloid Interface Sci.* **2001**, *241* (1), 178−187.
(20) Yessine, M.-A.; Lafleur, M.; Meier, C.; Petereit, H.-U.; Leroux, J.-C. Characterization of the Membrane-Destabilizing Properties of Different PH-Sensitive Methacrylic Acid Copolymers. *Biochim. Biophys. Acta, Biomembr.* **2003**, *1613* (1−2), 28−38, DOI: 10.1016/S0005-2736(03)00137-8.
(21) Leiske, M. N.; De Geest, B. G.; Hoogenboom, R. Impact of the Polymer Backbone Chemistry on Interactions of Amino-Acid-Derived Zwitterionic Polymers with Cells. *Bioact. Mater.* **2023**, *24* (January), 524−534.
(22) Wang, S.; Chen, R. PH-Responsive, Lysine-Based, Hyperbranched Polymers Mimicking Endosomolytic Cell-Penetrating Peptides for Efficient Intracellular Delivery. *Chem. Mater.* **2017**, *29* (14), 5806−5815.
(23) Chen, S.; Wang, S.; Kopytynski, M.; Bachelet, M.; Chen, R. Membrane-Anchoring, Comb-Like Pseudopeptides for Efficient, PH-Mediated Membrane Destabilization and Intracellular Delivery. *ACS Appl. Mater. Interfaces* **2017**, *9* (9), 8021−8029.
(24) Lehnen, A.-C.; Gurke, J.; Bapolisi, A. M.; Reifarth, M.; Bekir, M.; Hartlieb, M. Xanthate-Supported Photo-Iniferter (XPI)-RAFT Polymerization: Facile and Rapid Access to Complex Macromolecules. *Chem. Sci.* **2023**, *14* (3), 593−603.
(25) Martin, L.; Gody, G.; Perrier, S. Preparation of Complex Multiblock Copolymers via Aqueous RAFT Polymerization at Room Temperature. *Polym. Chem.* **2015**, *6* (27), 4875−4886.
(26) Mori, H.; Endo, T. Amino-Acid-Based Block Copolymers by RAFT Polymerization. *Macromol. Rapid Commun.* **2012**, *33* (13), 1090−1107.
(27) Leiske, M. N.; Singha, R.; Jana, S.; De Geest, B. G.; Hoogenboom, R. Amidation of Methyl Ester-Functionalised Poly(2-Oxazoline)s as a Powerful Tool to Create Dual PH- and Temperature-Responsive Polymers as Potential Drug Delivery Systems. *Polym. Chem.* **2023**, *14* (17), 2034−2044.
(28) Das, A.; Theato, P. Activated Ester Containing Polymers: Opportunities and Challenges for the Design of Functional Macromolecules. *Chem. Rev.* **2016**, *116* (3), 1434−1495.
(29) Singha, N. K.; Gibson, M. I.; Koiry, B. P.; Danial, M.; Klok, H. A. Side-Chain Peptide-Synthetic Polymer Conjugates via Tandem "Ester-Amide/Thiol-Ene" Post-Polymerization Modification of Poly(Pentafluorophenyl Methacrylate) Obtained Using ATRP. *Biomacromolecules* **2011**, *12* (8), 2908−2913.
(30) Gok, O.; Kosif, I.; Dispinar, T.; Gevrek, T. N.; Sanyal, R.; Sanyal, A. Design and Synthesis of Water-Soluble Multifunctionalizable Thiol-Reactive Polymeric Supports for Cellular Targeting. *Bioconjugate Chem.* **2015**, *26* (8), 1550−1560.
(31) Boyer, C.; Davis, T. P. One- Pot Synthesis and Biofunctionalization of Glycopolymers via RAFT Polymerization and Thiol−Ene Reactions. *Chem. Commun.* **2009**, No. 40, 6029−6031.
(32) Murata, H.; Prucker, O.; Rühe, J. Synthesis of Functionalized Polymer Monolayers from Active Ester Brushes. *Macromolecules* **2007**, *40* (15), 5497−5503.
(33) Moog, K. E.; Barz, M.; Bartneck, M.; Beceren-Braun, F.; Mohr, N.; Wu, Z.; Braun, L.; Dernedde, J.; Liehn, E. A.; Tacke, F.; Lammers, T.; Kunz, H.; Zentel, R. Polymeric Selectin Ligands Mimicking Complex Carbohydrates: From Selectin Binders to Modifiers of Macrophage Migration. *Angew. Chemie - Int. Ed.* **2017**, *56* (5), 1416−1421.
(34) Eberhardt, M.; Mruk, R.; Zentel, R.; Théato, P. Synthesis of Pentafluorophenyl(Meth)Acrylate Polymers: New Precursor Polymers for the Synthesis of Multifunctional Materials. *Eur. Polym. J.* **2005**, *41* (7), 1569−1575.
(35) Batz, H. G.; Franzmann, G.; Ringsdorf, H. Pharmakologisch Aktive Polymere, 5. Modellreaktionen Zur Umsetzung von Pharmaka Und Enzymen Mit Monomeren Und Polymeren Reaktiven Estern. *Die Makromol. Chemie* **1973**, *172* (1), 27−47.
(36) Ferruti, P.; Bettelli, A.; Feré, A. High Polymers of Acrylic and Methacrylic Esters of N-Hydroxysuccinimide as Polyacrylamide and Polymethacrylamide Precursors. *Polymer Guildf* **1972**, *13* (10), 462−464.
(37) Choi, J.; Schattling, P.; Jochum, F. D.; Pyun, J.; Char, K.; Theato, P. Functionalization and Patterning of Reactive Polymer Brushes Based on Surface Reversible Addition and Fragmentation Chain Transfer Polymerization. *J. Polym. Sci., Part A: Polym. Chem.* **2012**, *50* (19), 4010−4018.
(38) Kockelmann, J.; Zentel, R.; Nuhn, L. Post-Polymerization Modifications to Prepare Biomedical Nanocarriers with Varying Internal Structures, Their Properties and Impact on Protein Corona Formation. *Macromol. Chem. Phys.* **2023**, *224*, No. 2300199, DOI: 10.1002/macp.202300199.
(39) De Coen, R.; Vanparijs, N.; Risseeuw, M. D. P.; Lybaert, L.; Louage, B.; De Koker, S.; Kumar, V.; Grooten, J.; Taylor, L.; Ayres, N.; Van Calenbergh, S.; Nuhn, L.; De Geest, B. G. PH-Degradable Mannosylated Nanogels for Dendritic Cell Targeting. *Biomacromolecules* **2016**, *17* (7), 2479−2488.
(40) Duret, D.; Haftek-Terreau, Z.; Carretier, M.; Ladavière, C.; Charreyre, M.-T.; Favier, A. Fluorescent RAFT Polymers Bearing a Nitrilotriacetic Acid (NTA) Ligand at the α-Chain-End for the Site-Specific Labeling of Histidine-Tagged Proteins. *Polym. Chem.* **2017**, *8* (10), 1611−1615.
(41) Cepraga, C.; Gallavardin, T.; Marotte, S.; Lanoë, P. H.; Mulatier, J. C.; Lerouge, F.; Parola, S.; Lindgren, M.; Baldeck, P. L.; Marvel, J.; Maury, O.; Monnereau, C.; Favier, A.; Andraud, C.; Leverrier, Y.; Charreyre, M. T. Biocompatible Well-Defined Chromophore-Polymer Conjugates for Photodynamic Therapy and Two-Photon Imaging. *Polym. Chem.* **2013**, *4* (1), 61−67.
(42) Engler, A. C.; Chan, J. M. W.; Coady, D. J.; O'Brien, J. M.; Sardon, H.; Nelson, A.; Sanders, D. P.; Yang, Y. Y.; Hedrick, J. L. Accessing New Materials through Polymerization and Modification of a Polycarbonate with a Pendant Activated Ester. *Macromolecules* **2013**, *46* (4), 1283−1290.

(43) Smith, E.; Bai, J.; Oxenford, C.; Yang, J.; Somayaji, R.; Uludag, H. Conjugation of Arginine-Glycine-Aspartic Acid Peptides to Thermoreversible N-Isopropylacrylamide Polymers. *J. Polym. Sci., Part A: Polym. Chem.* **2003**, *41* (24), 3989−4000.
(44) Baessler, K. A.; Lee, Y.; Sampson, N. S. B1 Integrin Is an Adhesion Protein for Sperm Binding To Eggs. *ACS Chem. Biol.* **2009**, *4* (5), 357−366.
(45) Börner, H. G.; Sütterlin, R. I.; Theato, P.; Wiss, K. T. Topology-Dependent Swichability of Peptide Secondary Structures in Bioconjugates with Complex Architectures. *Macromol. Rapid Commun.* **2014**, *35* (2), 180−185.
(46) Nuhn, L.; Hartmann, S.; Palitzsch, B.; Gerlitzki, B.; Schmitt, E.; Zentel, R.; Kunz, H. Water-Soluble Polymers Coupled with Glycopeptide Antigens and T-Cell Epitopes as Potential Antitumor Vaccines. *Angew. Chem., Int. Ed.* **2013**, *52* (40), 10652−10656, DOI: 10.1002/anie.201304212.
(47) Leiske, M. N.; Kempe, K. A Guideline for the Synthesis of Amino-Acid-Functionalized Monomers and Their Polymerizations. *Macromol. Rapid Commun.* **2022**, *43* (2), 1−24.
(48) Maity, T.; Paul, S.; De, P. Side-Chain Amino Acid-Based Macromolecular Architectures. *J. Macromol. Sci. Part A* **2023**, *60* (1), 2−17.
(49) Leiske, M. N.; Mazrad, Z. A. I.; Zelcak, A.; Wahi, K.; Davis, T. P.; McCarroll, J. A.; Holst, J.; Kempe, K. Zwitterionic Amino Acid-Derived Polyacrylates as Smart Materials Exhibiting Cellular Specificity and Therapeutic Activity. *Biomacromolecules* **2022**, *23* (6), 2374−2387.
(50) Fujii, S.; Sakurai, K. Zwitterionic Amino Acid Polymer-Grafted Core-Crosslinked Particle toward Tumor Delivery. *Biomacromolecules* **2022**, *23* (9), 3968−3977.
(51) Koyama, E.; Sanda, F.; Endo, T. Syntheses and Radical Polymerizations of Methacrylamides Derived from Optically Active Amino Alcohols. *Macromol. Chem. Phys.* **1997**, *198* (11), 3699−3707.
(52) Yaşayan, G.; Redhead, M.; Magnusson, J. P.; Spain, S. G.; Allen, S.; Davies, M.; Alexander, C.; Fernández-Trillo, F. Well-Defined Polymeric Vesicles with High Stability and Modulation of Cell Uptake by a Simple Coating Protocol. *Polym. Chem.* **2012**, *3* (9), 2596−2604.
(53) Bou Zerdan, R.; Geng, Z.; Narupai, B.; Diaz, Y. J.; Bates, M. W.; Laitar, D. S.; Souvagya, B.; Van Dyk, A. K.; Hawker, C. J. Efficient Synthesis of Branched Poly(Acrylic Acid) Derivatives via Post-polymerization Modification. *J. Polym. Sci.* **2020**, *58* (14), 1989−1997.
(54) Hu, H.; Saniger, J.; Garcia-Alejandre, J.; Castaiio, V. M. Fourier Transform Infrared Spectroscopy Studies of the Reaction between Polyacrylic Acid and Metal Oxides. *Mater. Lett.* **1991**, *12*, 281−285, DOI: 10.1016/0167-577X(91)90014-W.
(55) Roy, S.; Mahali, K.; Mondal, S.; Dolui, B. K. Thermodynamics of DL-Alanine Solvation in Water-Dimethylsulfoxide Mixtures at 298.15 K. *Russ. J. Phys. Chem. A* **2015**, *89* (4), 654−662.
(56) Needham, T. E.; Paruta, A. N.; Gerraughty, R. J. Solubility of Amino Acids in Pure Solvent Systems. *J. Pharm. Sci.* **1971**, *60* (4), 565−567.
(57) Mahali, K.; Roy, S.; Dolui, B. K. Solubility and Solvation Thermodynamics of a Series of Homologous α-Amino Acids in Nonaqueous Binary Mixtures of Ethylene Glycol and Dimethyl Sulfoxide. *J. Chem. Eng. Data* **2015**, *60* (5), 1233−1241.
(58) Jochum, F. D.; Theato, P. Temperature- and Light-Responsive Polyacrylamides Prepared by a Double Polymer Analogous Reaction of Activated Ester Polymers. *Macromolecules* **2009**, *42* (16), 5941−5945.
(59) Chiantore, O. Polymer-Substrate Interactions in Size Exclusion Chromatography with Silica Gels and Pure Solvents. *J. Liq. Chromatogr.* **1984**, *7* (1), 1−11.
(60) Echeverria, C.; Peppas, N. A.; Mijangos, C. Novel Strategy for the Determination of UCST-like Microgels Network Structure: Effect on Swelling Behavior and Rheology. *Soft Matter* **2012**, *8* (2), 337−346.
(61) Jasinski, J.; Wilde, M. V.; Voelkl, M.; Jérôme, V.; Fröhlich, T.; Freitag, R.; Scheibel, T. Tailor-Made Protein Corona Formation on Polystyrene Microparticles and Its Effect on Epithelial Cell Uptake. *ACS Appl. Mater. Interfaces* **2022**, *14* (41), 47277−47287.
(62) Swieton, J.; Kaminski, K.; Miklosz, J.; Mogielnicki, A.; Kalaska, B. Anionic and Cationic Block Copolymers as Promising Modulators of Blood Coagulation. *Eur. Polym. J.* **2023**, *199*, No. 112452.
(63) Dailing, E. A.; Kilchrist, K. V.; Tierney, J. W.; Fletcher, R. B.; Evans, B. C.; Duvall, C. L. Modifying Cell Membranes with Anionic Polymer Amphiphiles Potentiates Intracellular Delivery of Cationic Peptides. *ACS Appl. Mater. Interfaces* **2020**, *12* (45), 50222−50235.
(64) Jiang, Z.; Liu, H.; He, H.; Yadava, N.; Chambers, J. J.; Thayumanavan, S. Anionic Polymers Promote Mitochondrial Targeting of Delocalized Lipophilic Cations. *Bioconjugate Chem.* **2020**, *31* (5), 1344−1353.
(65) Griffin, W. C. Classification of Surface-Active Agents by "HLB. *J. Cosmet. Sci.* **1949**, *1*, 311−326.
(66) Egan, R. W. Hydrophile-Lipophile Balance and Critical Micelle Concentration as Key Factors Influencing Surfactant Disruption of Mitochondrial Membranes. *J. Biol. Chem.* **1976**, *251* (14), 4442−4447.
(67) Rideal, E.; Taylor, F. H. On Haemolysis by Anionic Detergents. *Proc. R. Soc. London, Ser. B* **1957**, *146* (923), 225−241, DOI: 10.1098/rspb.1957.0007.
(68) Manaargadoo-Catin, M.; Ali-Cherif, A.; Pougnas, J.-L.; Perrin, C. Hemolysis by Surfactants—A Review. *Adv. Colloid Interface Sci.* **2016**, *228*, 1−16.
(69) Lichtenberg, D.; Robson, R. J.; Dennis, E. A. Solubilization of Phospholipids by Detergents Structural and Kinetic Aspects. *Biochim. Biophys. Acta, Rev. Biomembr.* **1983**, *737* (2), 285−304, DOI: 10.1016/0304-4157(83)90004-7.
(70) Bochicchio, D.; Panizon, E.; Monticelli, L.; Rossi, G. Interaction of Hydrophobic Polymers with Model Lipid Bilayers. *Sci. Rep.* **2017**, *7* (1), No. 6357, DOI: 10.1038/s41598-017-06668-0.
(71) Ohshima, H. A Simple Expression for Henry's Function for the Retardation Effect in Electrophoresis of Spherical Colloidal Particles. *J. Colloid Interface Sci.* **1994**, *168* (1), 269−271.
(72) Leiske, M. N.; Walker, J. A.; Zia, A.; Fletcher, N. L.; Thurecht, K. J.; Davis, T. P.; Kempe, K. Synthesis of Biscarboxylic Acid Functionalised EDTA Mimicking Polymers and Their Ability to Form Zr(Iv) Chelation Mediated Nanostructures. *Polym. Chem.* **2020**, *11* (16), 2799−2810.
(73) Richter, F.; Leer, K.; Martin, L.; Mapfumo, P.; Solomun, J. I.; Kuchenbrod, M. T.; Hoeppener, S.; Brendel, J. C.; Traeger, A. The Impact of Anionic Polymers on Gene Delivery: How Composition and Assembly Help Evading the Toxicity-Efficiency Dilemma. *J. Nanobiotechnol.* **2021**, *19* (1), 292.